Optical cavity modes in semicurved Fabry–Pérot resonators

Stéphane Mornet, Lionel Teule-Gay, David Talaga, Serge Ravaine, R.A.L. Vallée

RAPID COMMUNICATION | OCTOBER 25 2010

Optical cavity modes in semicurved Fabry–Pérot resonators

Stéphane Mornet; Lionel Teule-Gay; David Talaga; Serge Ravaine; Renaud A. L. Vallée

J. Appl. Phys. 108, 086109 (2010)
https://doi.org/10.1063/1.3493691

Optical cavity modes in semicurved Fabry–Pérot resonators

Stéphane Mornet,[1] Lionel Teule-Gay,[1] David Talaga,[2] Serge Ravaine,[3] and Renaud A. L. Vallée[3,a)]

[1]*Institut de Chimie de la Matière Condensée de Bordeaux, CNRS, Université Bordeaux I, 87 av. Dr A. Schweitzer, 33608 Pessac Cedex, France*

[2]*Institut des Sciences Moléculaires, Université Bordeaux I, 351 cours de la libération, 33405 Talence Cedex, France*

[3]*Centre de Recherche Paul Pascal (CNRS-UPR8641), 115 av. Dr A. Schweitzer, 33600 Pessac Cedex, France*

(Received 23 August 2010; accepted 24 August 2010; published online 25 October 2010)

We present a nanofabrication method which combines bottom-up and top-down techniques to realize nanosized curved Fabry–Pérot cavities. These cavities are made of a hexagonal closed packed monolayer of silica particles enclosed between flat and curved metallic mirrors. They exhibit geometric cavity modes such as those found in gold shell colloids. These modes manifest as dips in the reflection spectra which shift as a function of the diameter of the used nanoparticles. An excellent agreement is found between experiment and theory which allows us to properly interpret our data. The work presented here constitutes a further step to the development of curved photonics. © *2010 American Institute of Physics*. [doi:10.1063/1.3493691]

Noble metal structures with dimensions smaller than or comparable to the wavelength of light exhibit interesting optical properties due to the collective oscillation of conduction electrons (surface plasmons). In the case of small particles, this localized surface plasmon mode causes confinement of the electromagnetic field near the surface and leads to strong extinction in the visible and near infrared, depending on the geometry, size, and shape of the metal particle.[1,2] The enhanced local fields can be used to enhance the fluorescence emission,[3,4] the Raman signals,[5,6] or the photostability of luminescent dyes close to the metal surface by shortening the excited-state lifetime.[7–11] Beyond these noble metal nanoparticles, core-shell colloids, composed of a dielectric core surrounded by a metallic shell are particularly interesting to investigate. The plasmon frequency of these particles can be tuned throughout the visible and near-infrared part of the spectrum by varying either the core diameter or the shell thickness.[12–14] Besides these well-known collective extinction resonances the geometric cavity modes,[15,16] which result from the confinement of light inside the dielectric core while the cavity boundaries are determined by the metal shell, have not yet received much attention up to now.

In this letter, we aim to investigate such geometric cavity modes and demonstrate the possibility of designing efficient nano-optical devices, such as curved nanosized Fabry–Pérot resonators by a unique combination of sol-gel chemistry and top-down deposition techniques. The enhanced local field together with the focusing effect due to the curvature itself allows us to strengthen the cavity properties. The main features of such a cavity are analyzed numerically, using the finite-difference time-domain (FDTD) algorithm.

The optical cavities described here are obtained by deposition of a monolayer of monodisperse silica (SiO_2) particles arranged in a hexagonal closed packed (hcp) structure (dielectric layer) in between two reflecting slabs. The front mirror is a curved thin gold (Au) slab while the back mirror is either a silicon substrate (Si) or a thin gold-coated silicon substrate (Si+Au). Figure 1(a) shows the scheme of these two types of cavities. The gold layers, of 20 nm thickness, were deposited by reactive magnetron sputtering using pure Au (99.99%) target. The silica nanoparticles were synthesized following the Stöber–Fink–Bohn method[17] from tetraethoxysilane (Fluka) and ammonia (29% in water, J.T. Baker). The two-dimensional (2D) particle arrays were generated following the procedure previously described by Wang *et al.*[18] This procedure was applied for various sizes of silica nanoparticles ranging from 180 to 470 nm. The sputtering deposition parameters were set to get a reproducible deposition rate (around 12.5 nm min^{-1}), ensuring a good uniformity of the film thickness for all substrates. The optical properties of the cavities were investigated by reflection spectroscopy using a home-made system equipped with a deuterium tungsten–halogen fiber optic light source mikropack dh-2000 as sample excitation source. For collection, the reflected light was sent to a Horiba Jobin-Yvon HR800 spectrometer equipped with a 150 grooves mm^{-1} grating and a Symphony CCD detector providing a 2 nm resolution. In the spectra, the reflection signal was always normalized with respect to the corresponding one of either a pure silicon substrate or a 20 nm gold-coated silicon substrate. The FDTD simulations[19] were performed with a freely available software package.[20] The computational cell, in which the incoming wave propagates along the z direction with a linear polarization in the x direction, has been implemented with periodic boundary conditions in x and y directions and perfectly matched layers in the z direction. The dielectric permittivity of gold was specified by using the Drude–Lorentz model with parameters determined by Vial *et al.*,[21] based on the best fits, following a FDTD approach, to the relative permittivity of gold as tabulated by Johnson and Christy.[22]

a)Electronic mail: vallee@crpp-bordeaux.cnrs.fr.

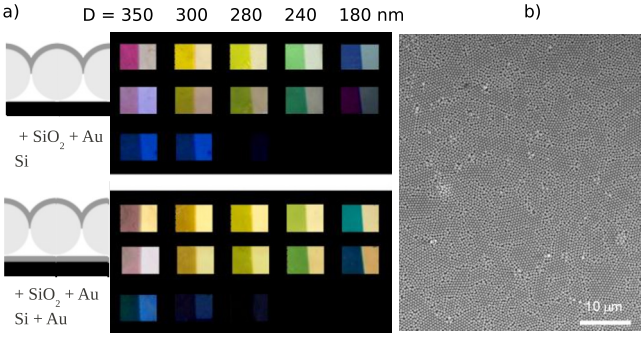

FIG. 1. (Color online) (a) Scheme of the designed cavities and photographs illustrating their change in color as a function of the increasing (from right to left) diameter D of the hcc-arranged particles and inclination of the samples with respect to the direction of acquisition (90°, 45°, 0° from top to bottom). The top (bottom) scheme pertains to silica (SiO_2) particles deposited on a pure silicon substrate (Si) [20 nm gold-coated silicon substrate (Si+Au)]. In both series, the right part of each sample has been masked before final gold sputtering. (b) SEM top view of a gold-coated monolayer of 470 nm silica particles.

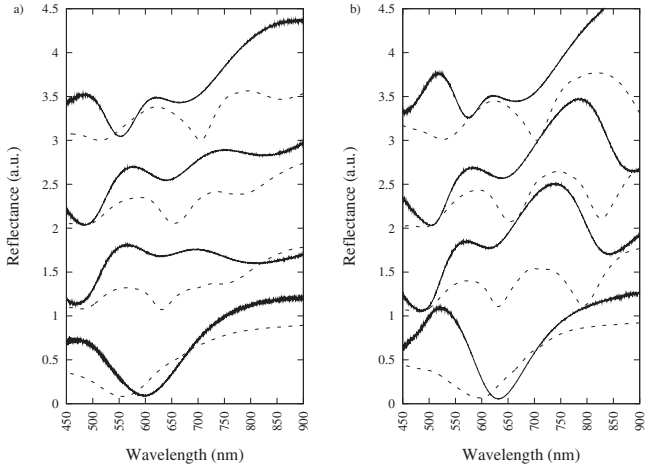

FIG. 2. Experimental (solid lines) and simulated (dashed lines) reflection spectra of the semicurved cavities for particles diameters D ranging from 180 nm to 240, 280, 300, and 350 nm, from bottom to top deposited either directly on the silicon wafer (a) or on the gold-coated silicon wafer (b). The spectra are offset by 1.0 from one another for visibility.

Figure 1(a) shows photographs of the various samples obtained with silica particles of diameter D decreasing from left $D=350$ nm to right $D=180$ nm. Two series are exhibited depending on whether the particles have been deposited directly on the silicon wafer (Si, top) or on the 20 nm thick gold-coated silicon wafer (Si+Au, bottom). In both cases, the considered structures have been closed (left part of each sample) with a thin gold film (Au, 20 nm thick), which adopted the curvature of the silica particles underneath, thus forming a semicurved cavity. A rich panel of colors is exhibited, depending on the diameter D of the silica particles. Furthermore, a progressive extinction is observed as the angle α is decreased from $\alpha=90°$ to $\alpha=0°$ (from top to bottom). The uniformity of the color areas extending on centimeter square can only be reached for perfectly designed micro/nanocavities, the quality of which is further exemplified in the scanning electron microscope (SEM) picture presented in Fig. 1(b).

In most cases, resonance in a nanostructure can be probed with far-field signals.[23] In this study, the entrance surfaces of the cavities were illuminated with a nearly collimated white light, and the backscattering spectrum was only measured from a selected area (50 μm) of each semicurved cavity. The measured quantity, hereafter simply called reflectance, is depicted in Fig. 2 (solid lines) as a function of wavelength and diameter of the silica particles deposited either directly on the silicon wafer (a) or on the gold-coated silicon wafer (b). Dips are observed in the reflection spectra and they systematically shift to the long wave range as a function of D. The same dips are observed while slightly shifted and with distinct amplitudes in case the used back mirror is either the pure silicon wafer or the gold-coated silicon wafer. The simulated reflection spectra (dashed lines) are superimposed on each figure. The good agreement between these spectra and the ones obtained experimentally is clearly observed and points to the usefulness of subsequent simulations to explain some behavioral characteristics.

Let us perform a close inspection to the case of silica particles with $D=300$ nm enclosed by the gold-coated silicon wafer and the front gold curved mirror. The usual interband transition exhibited by gold at around 500 nm manifests clearly as a dip in the reflectance [Fig. 2(b)]. It barely changes its position as a function of the cavity thickness. Besides this "pure" plasmonic resonance, the two extradips (at 654 nm and 828 nm, Fig. 2(b) exhibit a shift in their positions as a function of the cavity thickness, which is a clear sign of coupling of a cavity mode to some plasmonic collective oscillation. Furthermore, the simulated reflection and transmission spectra [Fig. 3(a)] of this structure exhibit some peculiar behavior: while the reflectance dip (detected at the entrance surface of the structure, Fig. 3, inset) shown at

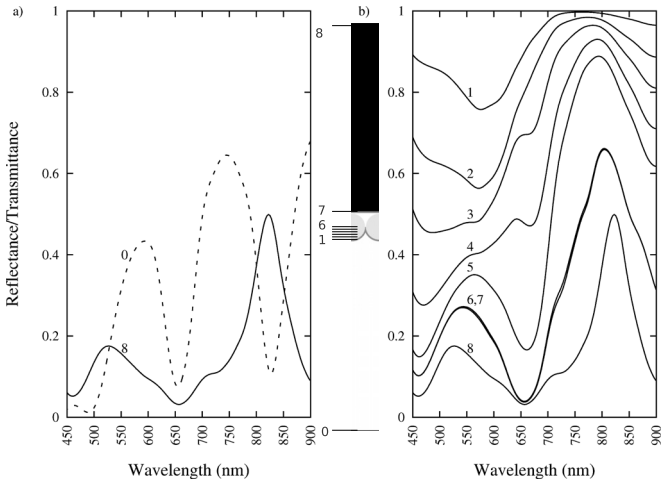

FIG. 3. (a) Simulated reflection (0, dashed) and transmission (8, solid) spectra of an array of hcp arranged monodisperse silica particles of diameter $D=300$ nm enclosed in between a front gold curved mirror and a gold-coated silicon wafer. (b) Simulated transmission spectra through flux planes situated at distances 5 (1), 30 (2), 50 (3), 70 (4), 90 nm (5) from the curved front mirror, in the center (6), at the back of the cavity (7) and at the outlet of the structure (8). Inset: geometry of the simulated structure with indication of the positions of the planes used for flux detection. The source originates from plane O and goes upwards. It is partially reflected/transmitted by the cavity. The reflected flux is detected back through plane O. The transmitted flux goes through the cavity, entering at the front mirror, is detected successively through planes 1 (5 nm after the front mirror) to 7 (back mirror) prior to continue through the substrate to be finally detected through plane 8 (outlet of the structure).

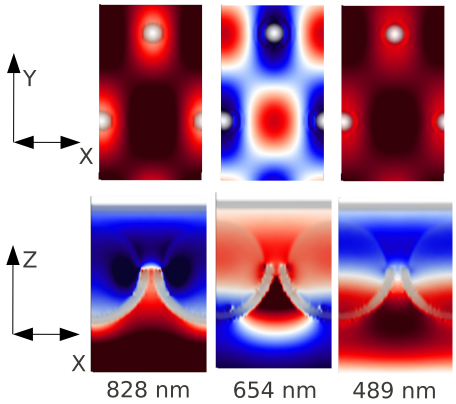

FIG. 4. (Color online) FDTD snapshots of the x-component of the electric field of a very narrow Gaussian pulse propagating in the z-direction of the curved cavity shown in Fig. 3. for wavelengths corresponding to the three reflectance dips observed.

828 nm coincides with a transmittance peak (detected at the outlet of the structure, Fig. 3, inset), the reflectance dip at 654 nm also exhibits a transmittance dip. Following the usual formula $T+R+A+Dif=1$, where T, R, A, and Dif stand for the transmittance, reflectance, absorbance, and diffusion, respectively, a minimum in both transmittance and reflectance clearly indicates a strongly absorbant and/or diffusive mode at 654 nm.

The fluxes transmitted through planes situated at various depths from the front gold curved mirror are presented in Fig. 3(b). Close to the front mirror (plane 1), a broad peak extending from about 600 nm to more than 900 nm emerges as a manifestation of a highly diffusing collective plasmon oscillation. As the distance from the front mirror increases, the extension of this peak reduces and it splits into two parts: a dip and a peak which reinforce and localize at $\lambda=654$ nm and $\lambda=828$ nm, respectively. The transmission spectra are almost indistinguishable as detected in the middle (plane 6) or at the back (plane 7) of the cavity. The behavior exhibited by the mode at $\lambda=654$ nm is reminiscent of a quadripolar plasmon resonance mode, mainly localized to the near field of the front mirror. The incoming light at that wavelength is completely absorbed/scattered by the front gold curved mirror and accordingly shows a dip in reflectance as in transmittance far from it. On the contrary, the mode at $\lambda=828$ nm. looks like a dipolar plasmon resonance mode, able to propagate on longer distances. The fact that these modes are coupled to the cavity is best illustrated by the shift they exhibit as a function of the cavity length (Fig. 2).

Finally, we simulated FDTD snapshots of the x-component of the electric field of a very narrow Gaussian pulse propagating in the z-direction of the structure shown in Fig. 3 for the three wavelengths of interest. The resonance at $\lambda=828$ nm clearly exhibits (Fig. 4) a dipolar character, very similar (while stronger) to the one of the interband transition at $\lambda=489$ nm. This indicates that this resonance is due to a cavity mode coupled to the dipolar collective mode. On the contrary, the FDTD snapshot (Fig. 4) corresponding to the dip at $\lambda=654$ nm is more quadripolar in nature and points to a resonance due to a cavity mode coupled to a collective quadripolar mode.

In conclusion, we have presented a simple nanofabrication method which combines bottom-up and top-down techniques to realize nanosized curved Fabry–Pérot cavities. These cavities exhibit geometrical cavity resonances that depend on the size of the dielectric core. Contrarily to our investigations, Yu *et al.*[24] reported the effect of the Al_2O_3 coating thickness on the reflectance properties of a similar structure. Owing to FDTD simulations, we could discriminate between dipolar and quadripolar resonances which result from the coupling of cavity modes and plasmonic collective modes. The strong exaltations observed (Fig. 4) in the vicinity of the front gold curved mirror are of particular interest: potential emitters could be inserted by functionalization at these positions and benefit of the maximum field. This feature could prove very important for applications as nanoscale light sources, sensors, or lasers. In this respect, the variation in the thickness of the metal shell will be a parameter of choice to increase the cavity quality factor.

Jean-Pierre Manaud (ICMCB) and Isabelle Ly (CRPP) are acknowledged for gold sputtering and SEM observations, respectively.

[1]U. Kreibig and M. Vollmer, *Optical Properties of Metal Clusters* (Springer, Berlin, 1995).
[2]C. F. Bohren and D. R. Huffman, *Absorption and Scattering of Light by Small Particles* (Wiley, New York, 1983).
[3]J. Gersten and A. Nitzan, J. Chem. Phys. **73**, 3023 (1980).
[4]J. S. Biteen, N. S. Lewis, H. A. Atwater, H. Mertens, and A. Polman, Appl. Phys. Lett. **88**, 131109 (2006).
[5]M. Moskovits, Rev. Mod. Phys. **57**, 783 (1985).
[6]J. B. Jackson and N. J. Halas, Proc. Natl. Acad. Sci. U.S.A. **101**, 17930 (2004).
[7]A. Parfenov, I. Gryczynski, J. Malicka, C. D. Geddes, and J. R. Lakowicz, J. Phys. Chem. B **107**, 8829 (2003).
[8]A. Moroz, Chem. Phys. **317**, 1 (2005).
[9]O. G. Tovmachenko, C. Graf, D. J. van den Heuvel, A. van Blaaderen, and H. C. Gerritsen, Adv. Mater. **18**, 91 (2006).
[10]J. Enderlein, Appl. Phys. Lett. **80**, 315 (2002).
[11]J. Enderlein, Phys. Chem. Chem. Phys. **4**, 2780 (2002).
[12]A. L. Aden and M. Kerker, J. Appl. Phys. **22**, 1242 (1951).
[13]A. E. Neeves and M. H. Birnboim, J. Opt. Soc. Am. B **6**, 787 (1989).
[14]S. J. Oldenburg, R. D. Averitt, S. L. Westcott, and N. J. Halas, Chem. Phys. Lett. **288**, 243 (1998).
[15]T. V. Teperik, V. V. Popov, and F. J. García de Abajo, Phys. Rev. B **69**, 155402 (2004).
[16]J. J. Penninkhof, L. A. Sweatlock, A. Moroz, H. A. Atwater, A. van Blaaderen, and A. Polman, J. Appl. Phys. **103**, 123105 (2008).
[17]W. Stöber, A. Fink, and E. Bohn, J. Colloid Interface Sci. **26**, 62 (1968).
[18]W. Wang, B. Gu, L. Liang, and W. Hamilton, J. Phys. Chem. B **107**, 3400 (2003).
[19]A. Taflove and S. C. Hagness, *Computational Electrodynamics: The Finite-Difference Time-Domain Method*, 3rd ed. (Artech House, Norwood, MA, 2005).
[20]A. F. Oskooi, D. Roundy, M. Ibanescu, P. Bermel, J. D. Joannopoulos, and S. G. Johnson, Comput. Phys. Commun. **181**, 687 (2010).
[21]A. Vial, A.-S. Grimault, D. Macías, D. Barchiesi, and M. Lamy de la Chapelle, Phys. Rev. B **71**, 085416 (2005).
[22]P. Johnson and R. Christy, Phys. Rev. B **6**, 4370 (1972).
[23]D. P. Fromm, A. Sundaramurthy, P. J. Schuck, G. Kino, and W. E. Moerner, Nano Lett. **4**, 957 (2004).
[24]X. Yu, L. Shi, D. Han, J. Zi, and P. V. Braun, Adv. Funct. Mater. **20**, 1 (2010).